

## An extension of the Planck galaxy cluster catalogue

R. A. Burenin\*

*Space Research Institute RAS, Moscow*

Received 20.11.2016

**Abstract** — We present a catalogue of galaxy clusters detected in the Planck all-sky Compton parameter maps and identified using data from the WISE and SDSS surveys. The catalogue comprises about 3000 clusters in the SDSS fields. We expect the completeness of this catalogue to be high for clusters with masses larger than  $M_{500} \approx 3 \times 10^{14} M_{\odot}$ , located at redshifts  $z < 0.7$ . At redshifts above  $z \approx 0.4$ , the catalogue contains approximately an order of magnitude more clusters than the 2nd Planck Catalogue of Sunyaev-Zeldovich sources in the same fields of the sky. This catalogue can be used for identification of massive galaxy clusters in future large cluster surveys, such as the SRG/eROSITA all-sky X-ray survey.

Key words: *galaxy clusters, sky surveys*

### INTRODUCTION

Measurement of the galaxy cluster mass function is one of the most sensitive methods used to constrain the parameters of the cosmological model (e.g., Vikhlinin et al., 2009a,b; Planck Collaboration, 2014a, 2016b). For such studies, large samples of massive galaxy clusters are needed.

One of the largest samples of massive galaxy clusters is the catalogue of clusters detected via the Sunyaev-Zeldovich (SZ) effect (Sunyaev, Zeldovich, 1972) in the Planck all-sky survey (Planck Collaboration, 2014b, 2016c). In this survey, the most massive clusters in the observable Universe are detected nearly uniformly over the entire extragalactic sky. The 2nd Planck Catalogue of SZ sources (PSZ2, Planck Collaboration, 2016c) contains 1653 objects, of which 1203 are confirmed massive galaxy clusters. Most of these clusters have masses larger than  $M_{500} \sim 6 \times 10^{14} M_{\odot}$ , i.e. they are the most massive clusters in the Universe. The number density of such objects is very small and their mass function is very steep.

Since the amplitude of the SZ effect depends mostly on galaxy cluster mass, lowering the detection limit in the Planck SZ survey should enable finding objects of lower mass, which would lead to a rapid increase in the number of detected clusters. For example, with a two times lower detection limit,  $M_{500} \sim 3 \times 10^{14} M_{\odot}$ , the number of detected clusters is expected to increase by an order of magnitude (e.g., Vikhlinin et al., 2009b). The cluster detection limit could be lowered if it were possible to use additional data for identification of clusters and elimination of false detections.

Below, we demonstrate that a useful sample of galaxy

clusters with masses above  $M_{500} \sim 3 \times 10^{14} M_{\odot}$  at redshifts  $z < 0.7$  can be obtained using the Planck all-sky Compton parameter maps in combination with data from the Wide-Field Infrared Survey Explorer (WISE) and Sloan Digital Sky Survey (SDSS). We present a catalogue of about 3000 galaxy clusters found using these data in the SDSS fields.

### SOURCE DETECTION IN PLANCK COMPTON PARAMETER MAPS

The detection of SZ sources in the Planck Collaboration catalogues was done using specialized procedures that take the spectral and spatial shape of the source into account (see, e.g., Planck Collaboration, 2016c). In addition, Compton parameter maps (y-maps) were constructed (Planck Collaboration, 2016a), which were mainly used for studying the angular power spectrum of the SZ signal. It has been demonstrated that there is a good agreement between the objects from the SZ source catalogue and the sources detected in the y-maps. Therefore, for simplicity, we have used the Planck Compton parameter maps to detect galaxy clusters.

We exploited maps of the Compton parameter and its standard deviation from the Planck 2015 data release (Planck Collaboration, 2016a), as provided by the Planck Legacy Archive<sup>1</sup>. We performed our source search using the NILC maps, because they have somewhat lower noise at small angular scales (see details in Planck Collaboration, 2016a). We smoothed the standard deviation map with a  $1^{\circ}$ -radius median filter. We then obtained a signal to noise map from the y-map and the smoothed standard deviation map and additionally subtracted large scale

\*e-mail: rodion@hea.iki.rssi.ru

<sup>1</sup><http://pla.esac.esa.int/>

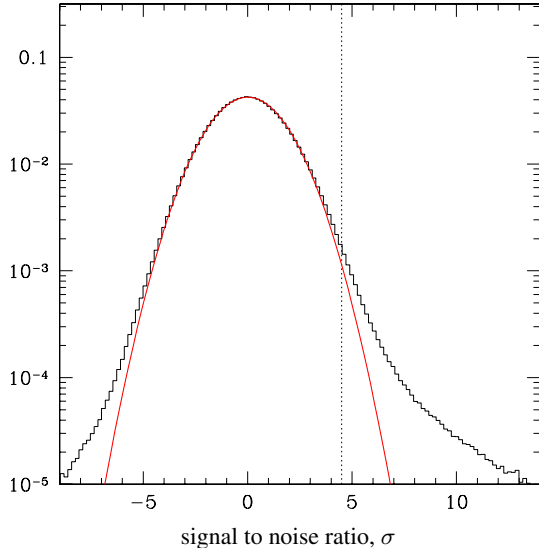


**Fig. 1.** Signal to noise ratio distribution of the  $y$ -parameter inside the Galactic foreground mask. The source detection threshold is shown with the dotted line.

anisotropy, which was estimated by smoothing the map with a  $1^\circ$ -radius median filter.

As a Galaxy foreground mask we used a mask produced by Khatri (2016). This mask makes allowance not only for Galaxy dust emission but also for the emission of carbon monoxide (CO), in particular in high-latitudes molecular clouds. The spectrum of the CO signal resembles the spectrum of  $y$ -distortions, so that CO emission significantly contaminates the Planck  $y$ -maps. Specifically, we used the 61% CO mask available in the public domain<sup>2</sup>.

Figure 1 shows the  $y$ -parameter signal to noise ratio distribution obtained as discussed above inside the Galactic foreground mask. Small deviations of the  $y$ -parameter from the mean value are well described by a Gaussian distribution, since the observed signal consists of instrumental noise and the averaged signal of a large number of faint SZ sources. At signal to noise ratios approximately  $> 5$ , the distribution differs significantly from the Gaussian one. Obviously, individual SZ sources start to appear above the noise level at these deviations from the mean value.

Since we use additional IR and optical data for cluster identification, which allows us to effectively eliminate false detections from the sample, we can use a lower source detection threshold to detect sources in the  $y$ -parameter map. We decided to use a  $4.5\sigma$  source detection threshold (shown with the dotted line in Fig. 1). Although a lot of projections of faint SZ sources may appear near this threshold, we expect to find also many real individual massive clusters, which can be identified using IR and optical data.

We considered only SZ sources inside the foreground mask discussed above. Also, only sources at Galactic lat-

itudes  $|b| > 20^\circ$  were considered, otherwise source identification in optical and IR bands would be difficult due to strong contamination from Galactic stars. We have thus selected 20290 SZ sources, of which 9227 are located in the SDSS fields. This number of detected sources indicates that the cluster mass threshold in our sample has been lowered not more than two times compared to the 2nd Planck Catalogue of SZ sources. Therefore, these sources (apart from the nearest ones) are not expected to be identified with clusters less massive than  $M_{500} \sim 3 \times 10^{14} M_\odot$ .

## IDENTIFICATION OF CLUSTERS IN THE OPTICAL AND INFRARED

### *The redMaPPer catalogue*

Galaxy clusters can be efficiently found using optical photometry, since most galaxies in clusters have similar colours and form the so-called red sequence in the colour-magnitude diagram (e.g., Gladders, Yee, 2000). To identify SZ sources detected in the Planck Compton parameter map, we used a galaxy cluster catalogue obtained from SDSS data using the *redMaPPer* cluster detection algorithm. Specifically, we used the publicly available *redMaPPer* catalogue, version 6.3<sup>3</sup>, which contains about 26000 galaxy clusters, all having relatively good photometric redshift and richness estimates. Cluster richness is known to correlate well with total cluster mass.

Since we are interested in massive galaxy clusters, with masses above  $M_{500} \sim 3 \times 10^{14} M_\odot$ , we considered only clusters with  $\lambda > 40$ , where  $\lambda$  is the cluster richness provided in the *redMaPPer* catalogue. This restriction allows us to reject low mass clusters but to keep nearly all clusters with masses  $M_{500} > 3 \times 10^{14} M_\odot$  included in the reference sample (Roza et al., 2015).

Figure 2 shows (red dashed line) the fraction of confirmed clusters from the PSZ2 catalogue that are detected in the SDSS fields using the *redMaPPer* algorithm (according to the version of the catalogue used here). We have applied the richness limit discussed above, but this has almost no effect on the number of identified clusters, as expected. Note that the *redMaPPer* mask has not been taken into account here, which may be one of the main reasons why the maximum identified fraction is less than 100%. We also see that the fraction of detected clusters drops at redshifts  $z > 0.55$ .

### *Clusters identified using WISE and SDSS data*

In order to more efficiently identify clusters at higher redshifts, we used IR data from the WISE survey in addition to SDSS optical data. The WISE all-sky survey (Wright et al., 2010) started in 2009 and was initially done in four photometric bands: 3.4, 4.6, 12 and 22  $\mu\text{m}$ . Since the end of the cryogenic phase in 2010, the survey has been continuing in the 3.4 and 4.6  $\mu\text{m}$  bands (Mainzer et al.,

<sup>2</sup><http://theory.tifr.res.in/~khatri/szresults/>

<sup>3</sup><http://risa.stanford.edu/redMaPPer/>

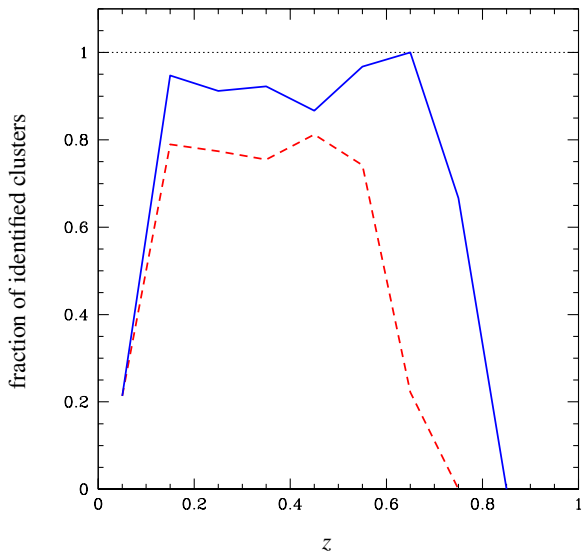


**Fig. 2.** Fraction of confirmed clusters from the PSZ2 catalogue in the SDSS fields that have also been detected with the *redMaPPer* algorithm (red dashed line, the *redMaPPer* mask is not taken into account) and with our new algorithm using WISE IR data (solid blue line).

2014). For galaxy cluster observations, the  $3.4 \mu\text{m}$  photometric band is most useful. In this band, distant galaxy clusters are well detected at redshifts up to  $z \approx 1-2$  (e.g., Burenin, 2015).

To search for galaxy clusters in the  $3.4 \mu\text{m}$  band images of the WISE all-sky survey, we used a completely automated algorithm that builds on the procedure described in our previous paper (Burenin, 2015). To detect clusters, we first subtracted stars from the WISE images, then detected extended IR sources in these images by convolving them with  $\beta$ -models of various angular sizes, and finally identified the brightest cluster galaxies and red sequences inside the detected IR sources using SDSS photometric data.

As compared to our earlier work cited above, the following improvements were made. We used more recent coadds of WISE and NEOWISE images, presented in Meisner et al. (2016) and available for public use<sup>4</sup> (see also, Lang, 2014). Flux measurements for the sources in WISE images were made using a more complete PSF model, taking into account not only its wings at large angular scales but also its angular asymmetry relative to its center. The data on source positions were taken from SDSS, data release 13 (SDSS Collaboration, 2017). Source flux fitting was done with frozen source positions in the sky, i.e. using so-called “forced photometry”. For brighter galaxies, where the form of the galaxy should be taken in account in addition to the PSF model, we used the “forced photometry” from Lang et al. (2016). In addition, we improved the red sequence detection procedure. The current version of this cluster detection algorithm is a preliminary one. We plan to further

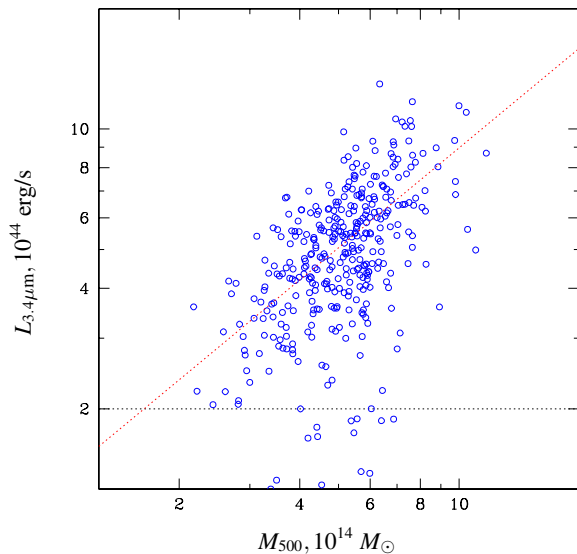


**Fig. 3.** Relation between the  $3.4 \mu\text{m}$  band luminosity inside the 1 Mpc radius and the total gravitational mass  $M_{500}$  of clusters from the PSZ2 catalogue.

improve it in the future, but even this preliminary version is suitable for identification of massive galaxy clusters among Planck SZ sources.

Since only massive clusters can appear among the SZ sources from the Planck survey, we should look for clusters with masses above  $M_{500} \sim 3 \times 10^{14} M_{\odot}$  in WISE images. In order to estimate galaxy cluster masses from IR data, cluster IR luminosities can be used (e.g., Lin et al., 2004; Kopylova, Kopylov, 2006). Figure 3 shows the correlation between the IR luminosity<sup>5</sup> in the  $3.4 \mu\text{m}$  band and the total mass  $M_{500}$  for clusters in the PSZ2 catalogue. The IR luminosity was calculated as the combined luminosity of red sequence galaxies within the 1 Mpc projected radius. The zero point and bandwidth calibrations were adopted from Jarrett et al. (2011). The K-corrections in the  $3.4 \mu\text{m}$  band were calculated using the 11 Gyr age synthetic stellar population model template taken from Bruzual, Charlot (2003), which appears to be a suitable model for all red sequence colours for clusters at redshifts  $z < 0.8$ .

We see from Fig. 3 that the cluster IR luminosity estimated in this way correlates well with the total cluster mass. The power law slope of this correlation is  $\approx 0.83 \pm 0.05$ . The slope is smaller than unity since the luminosity is calculated within a constant physical radius, rather than within a radius of constant density contrast. The scatter of the IR luminosity near this correlation, excluding larger than  $2.5\sigma$  deviations, is  $\sigma_{\ln L} = 0.25$  or  $\pm 29\%$ . Therefore, IR luminosities allow us to obtain total cluster mass estimates that are nearly as accurate as mass estimates obtained from cluster X-ray luminosities (Vikhlinin et al.,

<sup>5</sup>Hereafter, the cosmological model with  $\Omega_m = 0.3$ ,  $\Omega_{\Lambda} = 0.7$  and  $H_0 = 70 \text{ km } \ddot{\text{N}}\text{A}^{-1} \text{ Mpc}^{-1}$  is adopted.

<sup>4</sup><http://unwise.me/>

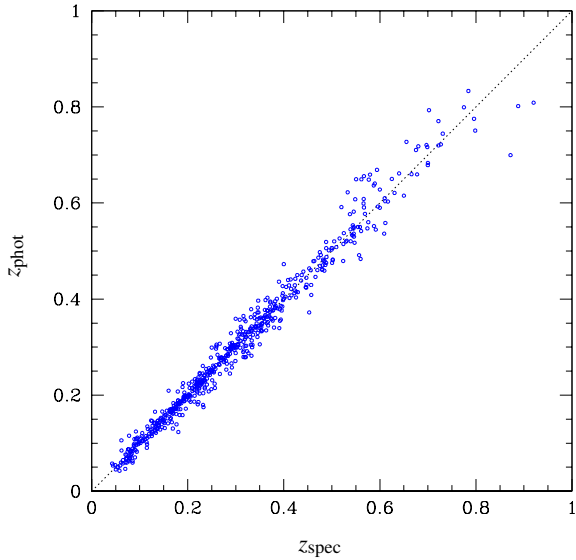


**Fig. 4.** Spectroscopic galaxy cluster redshifts vs. their photometric estimates from SDSS and WISE photometric data.

2009b) or optical richness (Rozo et al., 2015).

To identify clusters among Planck SZ sources, we used only clusters with IR luminosities  $L_{3.4\mu\text{m}} > 2 \times 10^{44} \text{ erg s}^{-1}$ . We see from Fig. 3 that most of the clusters with masses  $M_{500} > 3 \times 10^{14} M_{\odot}$  have IR luminosities above this limit. The fraction of confirmed clusters from the PSZ2 catalogue in the SDSS fields that are detected with our automated procedure, with the above IR luminosity constraint applied, is shown in Fig. 2 by the solid blue line. We see that nearly 90% of PSZ2 clusters at  $z > 0.1$  are detected using WISE data, while this fraction drops rapidly at  $z > 0.7$ . Therefore, we have managed to significantly increase the completeness of cluster identification at redshifts  $0.5 < z < 0.7$ , as compared to the *redMaPPer* catalogue.

Figure 4 compares photometric redshift estimates obtained with our automated cluster detection procedure with spectroscopic redshifts. These estimates were obtained using the cluster red sequence colours and the magnitudes of cluster brightest galaxies from SDSS and WISE photometric data. To calibrate our photometric estimates, we used clusters from the PSZ2 catalogue (Planck Collaboration, 2016c) as well as from the 400 square degree X-ray cluster survey (*400d*, Burenin et al., 2007) and the earlier 160 square degree cluster survey (*160d*, Vikhlinin et al., 1998) based on ROSAT pointings data. To increase the number of high redshift clusters at  $z > 0.6$ , five additional clusters were taken from the EMSS (Gioia, Luppino, 1994), WARPS (Perlman et al., 2002; Horner et al., 2008), MACS (Ebeling et al., 2001) and NEP (Henry et al., 2006) surveys, which are compiled in the MCXC catalogue (Piffaretti et al., 2011).

The accuracy of our photometric redshift estimation is  $\delta z_{\text{phot}}/(1+z) \approx 0.01$  at  $z < 0.5$  and  $\delta z_{\text{phot}}/(1+z) \approx 0.03$  at

$0.5 < z < 0.7$ . We see from Fig. 4 that our photometric redshift estimates, and therefore cluster IR luminosities, are not reliable at  $z > 0.7$ . Therefore, to identify Planck SZ sources, we use below only clusters with photometric redshift estimates  $z_{\text{phot}} < 0.7$ .

## THE CLUSTER CATALOGUE

As discussed above, there are 9227 SZ sources in the Planck Compton parameter map in the SDSS fields at  $|b| > 20$ , inside our Galaxy foreground map. We cross-correlated this sample with the following objects:

- objects from the 2nd Planck Catalogue of SZ sources (PSZ2, Planck Collaboration, 2016c);
- massive galaxy clusters from the *redMaPPer* catalogue (Rykoff et al., 2014);
- massive galaxy clusters detected in the fields of the SZ sources by our automated procedure using WISE and SDSS data.

As a result, we identified 2964 massive galaxy clusters with Planck SZ sources. Out of them, 483 clusters are present in the PSZ2 catalogue (see below), 1795 were identified using the *redMaPPer* catalogue and 2573 using WISE and SDSS data, as discussed above. Many clusters are identified with several methods. For example, 1459 clusters are identified both with the *redMaPPer* catalogue and using WISE and SDSS data.

Figure 5 shows the fraction of SZ sources identified with massive galaxy clusters as a function of the signal to noise ratio in the Planck  $y$ -parameter map. At low signal to noise ratios, only a small fraction of sources are identified with massive galaxy clusters. The other SZ sources are probably associated with non-gaussianities of the  $y$ -parameter maps, which are expected to arise due to projections of less massive clusters and groups of galaxies.

The catalogue of identified clusters is presented in Table 1, which provides the number of the source in the list, its coordinates ( $\alpha$ ,  $\delta$ , J2000), significance in the  $y$ -parameter map (S/N), the shift of the optical center relative to the center of the SZ source ( $\delta\alpha$ ,  $\delta\delta$  in arcminutes), cluster redshift ( $z$ ) and the number of galaxies used to obtain this redshift ( $N_z$ , see below for details). The last column of the Table gives the name of the source in the PSZ2 catalogue and indicates ambiguous identifications, in which case we identified the SZ source with the most massive cluster, as estimated from optical and IR data. The number of such projections in our sample is large, about 37%. Note that the fraction of projections for Planck SZ sources is relatively high even for bright SZ sources due the insufficient angular resolution of the Planck telescope (Planck Collaboration, 2013, 2015a).

**Table 1.** The cluster catalogue

Number	$\alpha$ (J2000)	$\delta$	S/N	$\delta\alpha$	$\delta\delta$	$z$	$N_c$	Note
				arc min				
1	00 00 48.9	+29 06 52	4.58	0.37	3.64	0.1928	3	
2	00 01 11.8	+21 33 49	7.77	-0.42	2.01	0.4110	5	PSZ2 G107.67-39.78
3	00 01 24.0	-00 00 53	4.55	-0.43	0.97	0.2479	5	
4	00 02 01.1	+12 03 28	9.52	0.62	-0.44	0.1989	17	PSZ2 G104.30-48.99
5	00 02 49.6	-01 04 06	4.99	-4.60	4.99	0.7600	1	**
6	00 02 47.9	-05 48 37	5.86	-3.21	4.33	0.4586	1	
7	00 03 06.0	-06 05 13	14.20	-1.48	0.47	0.2334	3	** PSZ2 G092.16-66.01
8	00 03 33.3	+10 02 17	6.10	-2.59	0.83	0.3707	4	
9	00 03 45.3	+02 04 55	7.21	-1.09	0.93	0.0924		** PSZ2 G099.57-58.64
10	00 04 01.1	+30 41 26	5.52	1.43	-0.96	0.7397	2	
11	00 03 58.1	-11 00 51	4.87	0.21	3.00	0.241*		
12	00 04 09.2	+04 35 54	5.36	-1.55	0.21	0.6396	1	
13	00 05 24.6	+16 11 23	7.22	-0.11	-1.81	0.1155	13	
14	00 06 16.1	-10 21 40	5.19	1.57	4.39	0.2180	1	**
15	00 06 21.4	+10 53 57	11.20	0.26	2.14	0.1669	15	PSZ2 G105.40-50.43
16	00 07 01.8	+25 05 02	5.64	1.36	-1.29	0.2409	2	
17	00 07 06.0	+10 34 21	4.83	-0.17	-0.26	0.1649	6	
18	00 07 27.4	+12 33 49	6.80	2.02	-3.61	0.697*		
19	00 08 12.4	+02 03 14	8.91	0.42	1.98	0.3651	3	PSZ2 G101.55-59.03
20	00 08 57.1	+13 06 46	4.68	-0.55	-0.26	0.195*		**
21	00 09 01.8	+32 10 09	5.42	2.26	-2.13	0.4790	2	
22	00 09 13.6	+03 56 18	4.83	-3.27	-3.06	0.1015	2	**
23	00 09 20.2	+06 49 06	10.04	-0.09	-0.34	0.2361	2	PSZ2 G104.71-54.54
24	00 09 42.4	+03 43 36	4.72	1.23	1.60	0.5622	2	
25	00 09 54.6	+12 17 28	8.18	-3.89	-0.63	0.1745	10	
26	00 09 59.7	+17 54 37	7.46	3.71	0.08	0.5583	2	
27	00 10 03.9	+25 52 01	7.46	0.08	-0.98	0.3211	6	**
28	00 10 08.0	+33 06 23	5.65	-0.15	-0.84	0.1136	1	**
29	00 10 13.5	+17 44 40	8.31	-1.42	0.47	0.1715	5	PSZ2 G109.22-44.01
30	00 10 18.2	+06 39 47	8.59	0.48	-0.75	0.2648	3	PSZ2 G104.98-54.79
31	00 10 26.6	+11 31 16	6.37	-2.58	1.32	0.0924	4	
32	00 10 48.4	+29 10 23	9.68	-1.09	0.50	0.3332	6	PSZ2 G112.35-32.86
33	00 10 50.8	-01 02 34	5.83	-3.54	-1.27	0.4646	1	**
34	00 10 56.0	+18 29 42	4.65	0.74	-2.00	0.5668	2	
35	00 11 45.5	+32 24 27	16.12	0.29	-1.04	0.1012	15	PSZ2 G113.29-29.69
36	00 12 13.5	+14 00 41	9.62	-0.39	-0.61	0.3895	2	PSZ2 G108.71-47.75
37	00 12 33.4	-00 16 23	5.07	0.86	-2.66	0.4027	2	
38	00 12 43.8	+06 08 08	5.26	-0.20	4.55	0.4310	1	
39	00 12 47.7	-08 58 27	8.86	-0.37	-2.76	0.3384	3	** PSZ2 G094.46-69.65
40	00 14 58.3	-00 55 06	6.03	1.14	2.08	0.5349	5	
...	...	...	...	...	...	...	...	

\* Photometric redshift estimate.

\*\* Two or more clusters at different redshifts are found in the SZ source field. The SZ source is identified with the cluster with the largest mass estimate from SDSS and WISE data.

Note. Only a small part of the Table is presented here for reference. The complete table contains 2964 lines and is available in the electronic version of the journal and also at <http://hea.iki.rssi.ru/psz/en/>

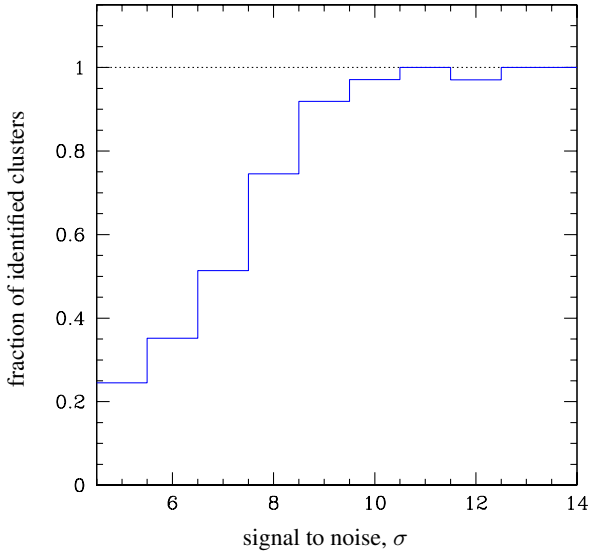


**Fig. 5.** Fraction of SZ sources identified with massive galaxy clusters as a function of the signal to noise ratio in the Planck  $y$ -parameter map.

#### The cluster redshifts

The cluster redshifts given in Table 1 in most cases are obtained from SDSS spectroscopic redshifts of galaxies. This is possible because brightest cluster galaxies are included in the samples of luminous red galaxies (LRG) that are observed spectroscopically in SDSS for studying baryon acoustic oscillations (Eisenstein et al., 2001). In addition, spectroscopy of cluster member galaxies for X-ray selected clusters (Clerc et al., 2016) has recently been started within SDSS.

For the SDSS based spectroscopic redshifts, Table 1 further provides the number of galaxies that were used to obtain the redshift of the cluster ( $N_z$ ). For these measurements, we selected galaxies at  $< 540$  kpc projected angular distances from the optical center of the cluster, whose spectroscopic redshifts are within the photometric redshift estimate uncertainty for the cluster. We then found the cluster spectroscopic redshift as the median value of the redshifts of these galaxies, having rejected  $\delta z > 0.01$  redshift deviations from the median. If the dispersion of the spectroscopic redshifts was too high and the median redshift value could not be obtained in this way, we adopted the photometric redshift estimate. Note that caution should be given to spectroscopic redshifts based on a small number of galaxies spectra, especially if there is no spectroscopic redshift for the brightest cluster galaxy. However, in most cases the accuracy and reliability of the spectroscopic redshifts is much higher than for the photometric redshift estimates.

It turns out that spectroscopic redshifts can be obtained from SDSS data for the majority of clusters in our catalogue, namely for 2541 clusters out of 2964. Figure 6 shows the redshift distribution of the clusters from the cat-

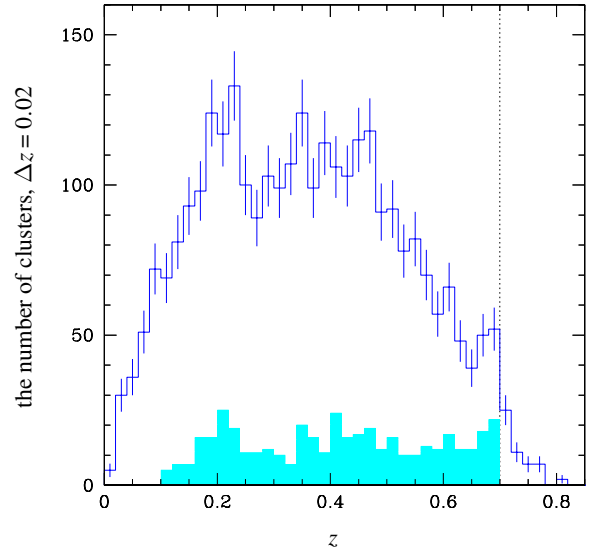


**Fig. 6.** Redshift distribution of identified clusters. The grey filled histogram shows the distribution of clusters without spectroscopic redshifts.

alogue. There are 423 clusters without spectroscopic redshifts in the catalogue. Their redshift distribution is shown in Fig. 6 with the grey filled histogram.

#### Clusters from PSZ2 catalogue

There are 1174 objects in the 2nd Planck Catalogue of Sunyaev-Zeldovich sources (PSZ2, Planck Collaboration, 2016c) at  $|b| > 20$ , inside the Galaxy foreground mask. Out of them, we detected 1135 objects in the Planck Compton parameter maps. Most of these sources are detected with a signal to noise ratio  $> 7$ .

We did not detect 39 objects from the PSZ2 catalogue in the Planck  $y$ -parameter map. Among these, *PSZ2 G006.84+50.69*, *PSZ2 G056.62+88.42*, *PSZ2 G061.75+88.11* and *PSZ2 G341.09-33.15* are located at the edges of very bright SZ sources — massive galaxy clusters A2029, Coma and A3667. The pair of sources *PSZ2 G096.77-50.29* and *PSZ2 G096.78-50.20* is located at an angular distance  $5.5'$  and is thus a duplicate.

We could not identify the reasons why the other PSZ2 sources are not detected in the  $y$ -parameter map. We note however that there are only three confirmed clusters among these sources. Moreover, the optical images of most of these sources reveal molecular clouds, which could produce a false SZ signal due to CO emission (Khatri, 2016). Therefore, almost all of the PSZ2 sources not included in our SZ source list are false ones or not confirmed as galaxy clusters.

There are 519 sources from the PSZ2 catalogue in the SDSS fields, inside our mask. Among them, 483 are identified with galaxy clusters in the optical and IR, as discussed above. Out of the remaining 36 sources, two sources (*PSZ2 G152.47+42.11* and *PSZ2 G199.73+36.98*) could be

identified with galaxy clusters with optical richness and IR luminosity lower than our thresholds. In addition, a few more clusters may be identified with distant clusters, located at  $z > 0.7$ . Currently we have only photometric redshift estimates for these clusters, and they are thus not included in our catalogue. The other SZ sources from this list cannot be confirmed as galaxy clusters using the available data.

Thus, about 93% of the sources from the PSZ2 catalogue that are also included in our SZ source list are confirmed as real galaxy clusters. This fraction is notably higher than the fraction of confirmed clusters in the PSZ2 catalogue (1203 out of 1653, i.e. about 73%). The reason is that we used a CO emission mask to exclude false detections (Khatri, 2016) and also that we confirmed 28 new clusters from the PSZ2 catalogue (see Table 1).

## DISCUSSION

We have found 2964 galaxy clusters in the SDSS fields at  $|b| > 20$ , inside the Galaxy foreground mask, while there are only 483 clusters in the 2nd Planck Catalogue of Sunyaev-Zeldovich sources (Planck Collaboration, 2016c) in the same area of the sky. The difference between the number of clusters in our list and in the PSZ2 catalogue is even higher for distant clusters. For example, there are 1218 clusters at  $z > 0.4$  in our catalogue, while there are only 97 clusters in the PSZ2 catalogue at these redshifts in the same regions of the sky. As discussed above, this is in agreement with the estimates of the lower mass limit for our catalogue,  $M_{500} \sim 3 \times 10^{14} M_{\odot}$  at high redshifts, which is approximately two times lower than for the PSZ2 catalogue.

Figure 7 shows an approximate range of masses and redshifts for clusters from our catalogue. For comparison, we show the masses and redshifts for clusters from the PSZ2 catalogue and lower limits for masses of clusters from the PSZ2 catalogue and the future SRG/eROSITA survey. The mass limit for the PSZ2 catalogue is adopted from Planck Collaboration (2016c) and that for the SRG/eROSITA survey has been calculated from its expected X-ray flux limit  $f_X > 3 \times 10^{-14} \text{ erg s}^{-1} \text{ cm}^{-2}$  (0.5–2 keV), using the mass – X-ray luminosity relation from Vikhlinin et al. (2009b). Note that for clusters with masses near  $3 \times 10^{14} M_{\odot}$ , a two times lower mass detection threshold corresponds to approximately an order of magnitude larger number of observed clusters.

We also note that the approximate lower mass limit for distant clusters from our catalogue,  $M_{500} > 3 \times 10^{14} M_{\odot}$ , corresponds to the masses of clusters that should be detected in the SRG/eROSITA survey at all redshifts (Churazov et al., 2015). We thus conclude that our catalogue contains a substantial fraction of the most massive clusters that will be discovered by SRG/eROSITA (see also Fig. 7). These clusters will be detected already during the first year of the SRG survey and will be included in

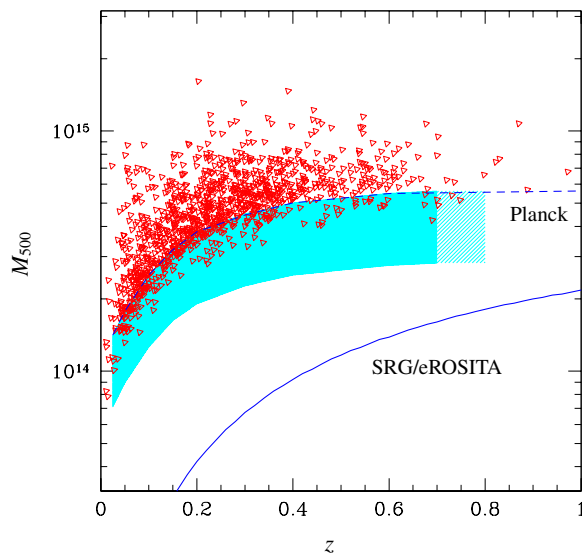


**Fig. 7.** The shaded area shows the approximate range of masses and redshifts for clusters from our catalogue. Red points show masses and redshifts for clusters from the PSZ2 catalogue (Planck Collaboration, 2016c). Also approximate lower limits for masses of clusters from the PSZ2 catalogue and the future SRG/eROSITA survey are shown with the dashed and solid lines, respectively.

all SRG/eROSITA cosmological samples and other large galaxy cluster surveys in the Northern sky.

We emphasize that we have found clusters near the detection limit of the Planck survey. Therefore, a significant number of clusters can be missed in our catalogue near its supposed mass threshold. Moreover, the angular resolution of the Planck telescope is in fact insufficient for detection of distant clusters with masses near  $3 \times 10^{14} M_{\odot}$ . For this reason, our catalog contains a large number of projections (about 37%), which are impossible to resolve with the Planck telescope. Therefore, the quality of our catalogue is not high and it would be difficult to obtain any cosmological constraints using this cluster sample. However, our catalogue can be used to identify massive galaxy clusters that will be discovered in future large cluster surveys, such as the planned SRG/eROSITA all-sky X-ray survey.

## CONCLUSIONS

We present a catalogue of galaxy clusters detected in Planck all-sky Compton parameter maps and identified using data from the WISE and SDSS surveys. Our catalogue comprises about 3000 clusters found in the SDSS fields, with masses higher than approximately  $M_{500} \sim 3 \times 10^{14} M_{\odot}$ . At redshifts above  $z \approx 0.4$ , the catalogue contains approximately an order of magnitude more clusters than the 2nd Planck Catalogue of Sunyaev-Zeldovich sources in the same fields of the sky. Therefore, much more galaxy clusters can be discovered using the Planck survey data, as compared to the number of clusters in the PSZ2 catalogue. This is in agreement with the results obtained recently by

Hurier et al. (2017), who found more SZ sources in Planck survey data with the improved SZ sources detection algorithm.

In our work, clusters were found near the detection limit of the Planck  $\gamma$ -parameter map. Moreover, due to the insufficiently high angular resolution of the Planck telescope, there is a large number of projections in our catalogue (about 37%). Therefore, the quality of our catalogue is not high. However, this catalogue can be used to identify massive galaxy clusters in large cluster surveys, such as the upcoming SRG/eROSITA all-sky X-ray survey.

The majority of clusters in our catalogue already have spectroscopic measurements of their redshifts. The number of the remaining clusters (about 400) is not high, so that their redshifts can be measured at ground telescopes equipped with efficient low-resolution spectrographs. Our group has been carrying out optical identifications and redshift measurements for galaxy clusters from Planck surveys using various ground telescopes (Planck Collaboration, 2015a,b, 2016d; Vorobyev et al., 2016). To perform these observations, we have access to a significant amount of observing time at the Russian-Turkish 1.5-m telescope, the 6-m telescope of SAO RAS (BTA), and the 1.6-m Sayan Observatory telescope, which has recently been equipped with a new medium and low resolution spectrograph (Burenin et al., 2016). We thus hope to measure all of the missing spectroscopic redshifts in our cluster catalogue before the launch of the SRG space observatory.

The author is grateful to R. Khatri for the detailed discussions of his results and for very useful CO emission masks available for public use. This work has been supported by Russian Science Foundation grant 14-22-00271.

#### REFERENCES

1. R.A. Burenin, A. Vikhlinin, A. Hornstrup, H. Ebeling, H. Quintana, A. Mescheryakov, *Astrophys. J. Suppl. Ser.* **172**, 561 (2007).
2. R.A. Burenin, *Astronomy Letters* **41**, 167 (2015).
3. R.A. Burenin, A.L. Amvrosov, M.V. Eselevich, V.M. Grigor'ev, V.A. Aref'ev, V.S. Vorob'ev, et al., *Astronomy Letters* **42**, 295 (2016).
4. G. Bruzual and S. Charlot, *Mon. Not. R. Astron. Soc.* **344**, 1000 (2003).
5. N. Clerc, A. Merloni, Y.-Y. Zhang, A. Finoguenov, T. Dwelly, K. Nandra, et al., *Mon. Not. R. Astron. Soc.* **463**, 4490 (2016).
6. E. Churazov, A. Vikhlinin and R. Sunyaev, *Mon. Not. R. Astron. Soc.* **450**, 1984 (2015).
7. H. Ebeling, A.C. Edge and J.P. Henry, *Astrophys. J.* **533**, 668 (2001).
8. D.J. Eisenstein, J. Annis, J.E. Gunn, A.S. Szalay, A.J. Connolly, R.C. Nichol, et al., *Astron. J.* **122**, 2267 (2001).
9. I.M. Gioia and G.A. Luppino, *Astrophys. J. Suppl. Ser.* **94**, 583 (1994).
10. M.D. Gladders and H.K.C. Yee, *Astron. J.* **120**, 2148 (2000).
11. J.P. Henry, C.R. Mullis, W. Voges, et al., *Astrophys. J. Suppl. Ser.* **162**, 304 (2006).
12. D.J. Horner, E.S. Perlman, H. Ebeling, et al., *Astrophys. J. Suppl. Ser.* **176**, 374 (2008).
13. G. Hurier, N. Aghanim and M. Douspis, arXiv:1702.00075.
14. T.H. Jarrett, M. Cohen, F. Masci, E. Wright, D. Stern, D. Benford, et al., *Astrophys. J.* **735**, 112 (2011).
15. R. Khatri, *Astron. Astrophys.* **592**, A48 (2016).
16. F.G. Kopylova, A.I. Kopylov, *Astronomy Letters* **32**, 84 (2006).
17. D. Lang, *Astron. J.* **147**, 108 (2014).
18. D. Lang, D.W. Hogg and D.J. Schlegel, *Astron. J.* **151**, 36 (2016).
19. Y.-T. Lin, J.J. Mohr, and S.A. Stanford, *Astrophys. J.* **610**, 745 (2004).
20. A. Mainzer, J. Bauer, R.M. Cutri, T. Grav, J. Masiero, R. Beck, P. Clarkson, et al., *Astrophys. J.* **792**, 30 (2014).
21. A.M. Meisner, D. Lang and D.J.A. Schlegel, arXiv:1603.05664.
22. E.S. Perlman, D.J. Horner, L.R. Jones, et al., *Astrophys. J. Suppl. Ser.* **140**, 265 (2002).
23. R. Piffaretti, M. Arnaud, G.W. Pratt, E. Pointecouteau and J.-B. Melin, *Astron. Astrophys.* **534**, A109 (2011).
24. Planck Collaboration: P.A.R. Ade, N. Aghanim, M. Arnaud, et al. (Planck Intermediate Results IV), *Astron. Astrophys.* **550**, A130 (2013).
25. Planck Collaboration: P.A.R. Ade, N. Aghanim, C. Armitage-Caplan, et al. (Planck 2013 Results XX), *Astron. Astrophys.* **571**, A20 (2014a).
26. Planck Collaboration: P.A.R. Ade, N. Aghanim, C. Armitage-Caplan, et al. (Planck 2013 Results XXIX), *Astron. Astrophys.* **571**, A29 (2014b); arXiv:1303.5089.
27. Planck Collaboration: P.A.R. Ade, N. Aghanim, M. Arnaud et al. (Planck Intermediate Results XXVI:), *Astron. Astrophys.* **582**, A29 (2015a); arXiv:1407.6663.
28. Planck Collaboration: P.A.R. Ade, N. Aghanim, C. Armitage-Caplan, et al. (Planck 2013 Results XXXII), *Astron. Astrophys.* **581**, A14 (2015b); arXiv:1502.00543.
29. Planck Collaboration: N. Aghanim, M. Arnaud, M. Ashdown, et al. (Planck 2015 Results XXIV), *Astron. Astrophys.* **594**, A24 (2016a); arXiv:1502.01597.
30. Planck Collaboration: P.A.R. Ade, N. Aghanim, M. Arnaud et al. (Planck 2015 Results XXIV), *Astron. Astrophys.* **594**, A24 (2016b); arXiv:1502.01597.
31. Planck Collaboration: P.A.R. Ade, N. Aghanim, M. Arnaud et al. (Planck 2015 Results XXVII), *Astron. Astrophys.* **594**, A27 (2016c); arXiv:1502.01598.
32. Planck Collaboration: P.A.R. Ade, N. Aghanim, M. Arnaud et al. (Planck Intermediate Results XXXVI), *Astron. Astrophys.* **586**, A139 (2016d); arXiv:1504.04583.
33. E. Rozo, E.S. Rykoff, J.G. Bartlett and J.-B. Melin, *Mon. Not. R. Astron. Soc.* **450**, 592 (2015).
34. E.S. Rykoff, E. Rozo, M.T. Busha, C.E. Cunha, A. Finoguenov, A. Evrad, et al., *Astrophys. J.* **785**, 104 (2014).



35. SDSS Collaboration: F.D. Albareti, C.A. Prieto, A. Almeida, et al., *Astrophys. J. Suppl. Ser.*, in press (2017); arXiv:1608.02013.
36. R.A. Sunyaev and Ya.B. Zeldovich, *Comments on Astrophysics and Space Physics*, **4**, 173 (1972).
37. A. Vikhlinin, B.R. Mcnamara, W. Forman, C. Jones, H. Quintana and A. Hornstrup, *Astrophys. J.* **502**, 558 (1998).
38. A. Vikhlinin, R.A. Burenin, H. Ebeling, W.R. Forman, A. Hornstrup, C. Jones, A.V. Kravtsov, S.S. Murray, et al., *Astrophys. J.* **692**, 1033 (2009a).
39. A. Vikhlinin, A.V. Kravtsov, R.A. Burenin, H. Ebeling, W.R. Forman, A. Hornstrup, C. Jones, S.S. Murray, et al., *Astrophys. J.* **692**, 1060 (2009b).
40. V.S. Vorobyev, R.A. Burenin, I.F. Bikmaev, I.M. Khamitov, S.N. Dodonov, R.Ya. Zhuchkov, et al., *Astronomy Letters* **42**, 63 (2016).
41. E.L. Wright, P.R.M. Eisenhardt, A.K. Mainzer, M.E. Ressler, R.M. Cutri, T. Jarrett, J.D. Kirkpatrick, D. Padgett, et al., *Astron. J.* **140**, 1868 (2010).